Short Communication

Growth Mechanism and Morphologies Tuning of ZnO Nanostructures

Wei Zhang[*], *Peng Wang, Xuening Fei, Yan Xiu and Guozhi Jia*

Tianjin Chengjian University, Tianjin300384, China
[*]E-mail: zhangwei001@tcu.edu.cn

A variety of morphologies of ZnO nanostructure powders were successfully fabricated by chemical bath deposition (CBD) technique at a low temperature. The structure and morphology of the ZnO products were observed by scanning electron microscopy. The investigation demonstrated that the ZnO nanostructures showing the hexagonal wurtzite structure. The aspect ratio of ZnO nanorods decrease with the equimolar increasing of the reactants. The ZnO nanostructures show different morphologies with the increasing of the concentration when the reactant concentration is not equal. The forming mechanism of the ZnO nanostructures was discussed in detail.

1. INTRODUCTION

The controllable growth of nanostructure is an important topic in the field of nanoscience. Recently, more attention was paid to ZnO nanostructure owing to its potential advantages and a wide range of applications. ZnO is a II-VI direct wide band gap semiconductor material, whose band gap is 3.37 eV at room temperature, and the exciton binding energy as high as 60 meV. ZnO nanomaterials are often used in the preparation of the UV detector, solar cells[1], optoelectronic devices and light emitting devices[2] due to the unique structural characteristics. ZnO nano materials can be applied in light weight materials and low-cost electrode materials for solar cells[3]. Electrochemically deposited nanoporous ZnO on FTO electrode has been studied in the photoelectrode [4]. Recently, the electrochemical synthesis of nanostructured ZnO films prepared from zinc nitrate aqueous solutions is reported[5]. More and more researchers successfully prepared various morphology of ZnO one-dimensional nanostructures, including nanorods, nanoflowers, nanoplates, nanotubes[6] and nanopins. As for the preparation method of ZnO nanostructures, there are an amount of techniques used to synthesize ZnO nanostructures. For example, metal-organic chemical vapor

deposition (MOCVD) [7], pulsed laser deposition[8], magnetron sputtering method[9], chemical bath deposition (CBD), electrochemically deposited ZnO thin films and so on. CBD has been applied more broadly because it is a simple method in aqueous solution and grown in low temperature. In addition, CBD have another outstanding characteristics, such as the simplicity of operation, the low cost, and so forth[10]. Jia et al successfully prepared controlled ZnO nanorods arrays on different substrates using sol-gel and chemical bath deposition technique, and investigate the important effect of strain[11-12]. Wang et al prepared large-scale ZnO arrays with vary of morphologies, including tower-like, flower-like, etc. by a chemical solution route and deeply discussed the growth mechanism [13].

In recent years, the preparation of ZnO nanomaterials by CBD has become the focus of the researchers, but most researchers concentrated on controlling the size of particles, only a few reports described the forming mechanism of the morphology. In this paper, we employ CBD technique to grow ZnO nanostructures with different morphologies and explore the effect of the reactant concentration on the morphology prosperities. In addition, we make a preliminary discussion of the growth mechanism.

2. EXPERIMENT

All reagents used in this experiment, including zincacetate dehydrate $Zn(CH_3COO)_2 \cdot 2H_2O$, hexamethylenetetramine ($C_6H_{12}N_4$), were analytically pure and used as purchased without further purification. All solutions were prepared with deionized water.

The synthetic procedure for fabricating ZnO nanopowders by CBD technique was composed as follows: (1) Equimolar amount $Zn(CH_3COO)_2 \cdot 2H_2O$ and $C_6H_{12}N_4$ (0.01,0.02,0.03mol/L, respectively) were dissolved into the 80mL deionized water; (2) The concentration of $C_6H_{12}N_4$ was kept constant at 0.01 mol/L while the concentration of the $Zn(CH_3COO)_2 \cdot 2H_2O$ was varied from 0.01 mol/L to 0.03 mol/L; (3)The concentration of $C_6H_{12}N_4$ was maintained at 0.04mol/L, while the concentration of $Zn(CH_3COO)_2 \cdot 2H_2O$ changed from 0.01mol/L to 0.03 mol/L. All the above mixed solution was stirred at room temperature for several minutes until formed a homogeneous solution. Next, the temperature of the solution was gradually increased to 90 ^{0}C with the magnetic stirring, and stayed for 1 hour. After a period of growth, ZnO nanorods would be generated in the bottom of beaker. After the reaction was completed, the solution was cooled to room temperature, and then the reaction solution was washed with deionized water and ethanol for several times. Finally, the product will be dried in air until the powder is formed. The general morphology properties and superficial characteristics of the as-prepared ZnO nanorods powders were examined by scanning electron microscopy (SEM) using a SHIMADZU SS-550 microscopy with 30kV.

3. RESULTS AND DISCUSSION

The preparation of ZnO nanorods was the pure wurtzite structure. Fig. 1(a), (b), (c) and (d) show the surface morphology of the ZnO nanostructures grown with different concentrations: 0.01mol/L, 0.02mol/L, 0.03mol/L and 0.04mol/L, respectively. The length of the scale bars is 2μm.
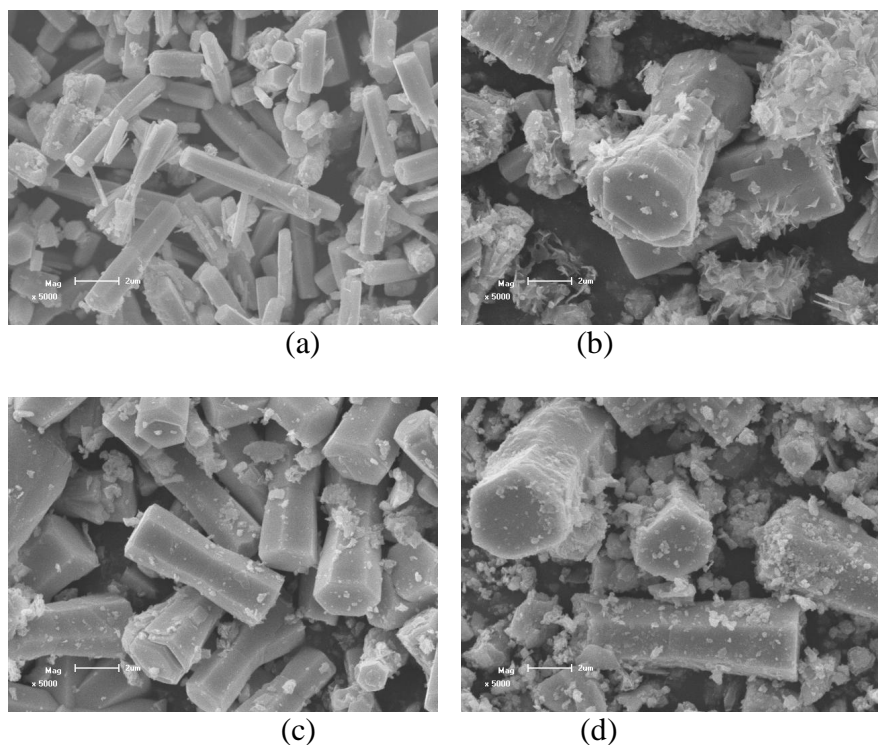
Figure 1. SEM photographs of ZnO nanorods grown with different solution concentration. (a) 0.01, 0.01mol/L; (b) 0.02, 0.02mol/L; (c) 0.03, 0.03mol/L; (d) 0.04, 0.04mol/L; The length of the scale bars is 2µm.
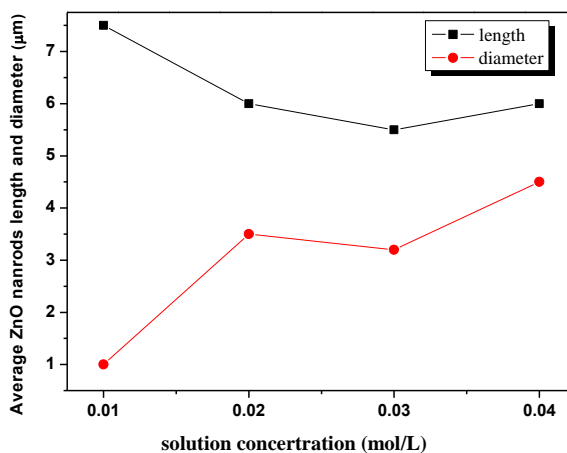

Figure 2. Average length and diameter of ZnO nanorods grown in different solution concentration.

It can be seen from the fig 2, the concentration had a great influence on the morphology of the ZnO nanorods. The general length of the ZnO crystals is 7.5µm and the average diameter is 1µm when the reactant concentration is 0.01mol/L. With the increasing of $Zn(CH_3COO)_2 \cdot 2H_2O$ and $C_6H_{12}N_4$ equimolarly, the length of ZnO nanorods showing the trend of reduced, while the diameter increased gradually, the length and diameter are about 6.5µm, 5.5µm, 6µm and 3.5µm, 3µm, 4.5µm, respectively shown in fig 2. From the figure, it can be seen that the aspect ratio of ZnO nanorods was gradually

decreased and the specific surface area was gradually increased with the increasing of the concentration of reactants equimolarly. Therefore, it can be concluded that the sizes of ZnO nanorods depend on the concentration of reactants, which can lead to the products with different length and diameters.

The grown mechanism of ZnO nanorods in this experiment was relevant with the reported before which explain the formation of several multi-branched ZnO nanoclusters. Gao et al reported that the morphology of the ZnO nanorods depends largely on the effect of selective dissolution etching [17]. In addition, other relevant reports involve the morphology of ZnO nanostructure changed depending on the polymers such as the shape of ring-like morphology [18]. In general, the wurtzite ZnO crystal has two polar planes: the low index planes that have high surface energy and in the metastable status. In addition, with the wurtzite hexagonal crystal structure, the six crystallographic equivalent nonpolar planes, which parallel to the c-axis, are more stable due to relatively low surface energy [19]. The formation of various shapes of ZnO nanocrystals is originated in the relative growth rates of different crystal facets. It is have a large difference for the growth rates of the wurtzite hexagonal ZnO crystals in different directions under hydrothemal conditions [20]. According to the lowest energy principle, hexagonal ZnO crystals are inclined to grow along the [0001] facet to achieve the surface energy minimization, hence the growth velocity along the [0001] direction is faster than other growth facets, which lead to the formation of nanorods along the c-axis. In this experiment, the morphology of ZnO nanostructure can be tuned by changing the growth parameters such as ion concentration, and the size and length of ZnO nanorods can be easily controlled during the process of chemical bath deposition.
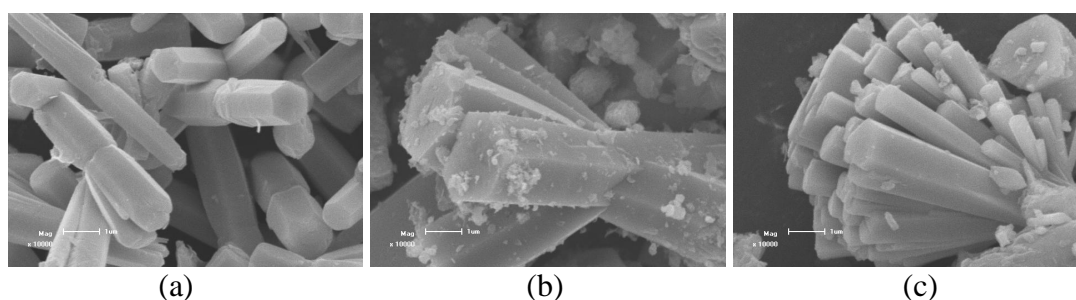

(a) (b) (c)
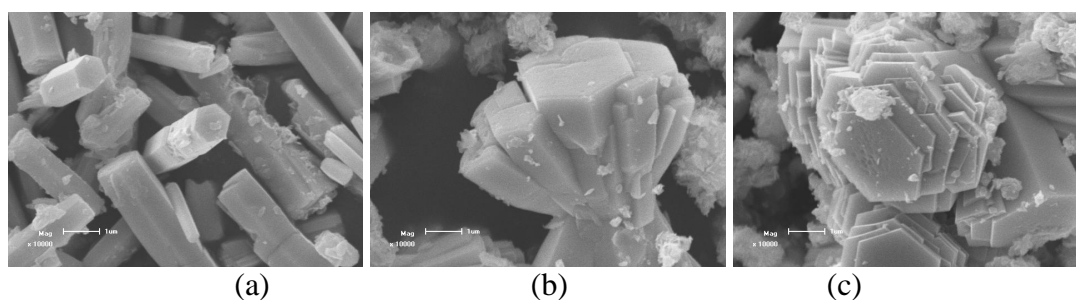
Figure 3. SEM photographs of ZnO nanorods grown with different solution concentration of $C_6H_{12}N_4$ and $Zn(CH_3COO)_2 \cdot 2H_2O$: (a) 0.01, 0.01mol/L; (b) 0.01, 0.02mol/L; (c) 0.01, 0.03mol/L; The length of the scale bars is 2μm.

Fig. 3 showed the images of the different ZnO nanostructure with the changes of the concentration of $Zn(CH_3COO)_2 \cdot 2H_2O$ and $C_6H_{12}N_4$ as (a)0.01, 0.01mol/L; (b) 0.01, 0.02mol/L; (c) 0.01, 0.03mol/L), respectively. It can be seen from the figure, the morphologies of ZnO were affected by the concentration extremely. The dumbbell-shaped ZnO nanostructures were formed with the increasing of the concentration. In addition, the cluster-like ZnO complex nanostructures were formed with further increasing of the concentration ratio. These observations through the above images

clearly reflect that the length and diameter of the obtained ZnO nanostructures also increased with increasing of the reactant concentration ratio.

The shape of dumbbell-shaped and cluster-like of ZnO nanostructures depends on the amount of the concentration of Zn^{2+}. When the Zn^{2+} concentration was high, a lot of ZnO nuclei are generated and grew into ZnO nanorods. The morphology of nanostructure can be controlled by tuning the concentration of Zn^{2+}. Therefore, it should be noted that the morphology of ZnO nanorods can be tuned by changing the ratio of $Zn(CH_3COO)_2 \cdot 2H_2O$ and $C_6H_{12}N_4$ in the solution, which implied that ZnO nuclei were formed in the solution, then were adsorbed or deposited to the glass substrate[8]. When $Zn(CH_3COO)_2 \cdot 2H_2O$ at a higher concentration, a large number of ZnO nuclei can be generated. Besides, there is no substrate in the beaker, which causes part of the ZnO nuclear reunion together and finally dumbbell-like and cluster-like ZnO nanostructures were formed.

(a)   (b)   (c)

Figure 4. SEM photographs of ZnO nanorods grown with different solution concentration of $C_6H_{12}N_4$ and $Zn(CH_3COO)_2 \cdot 2H_2O$: (a) 0.04, 0.01mol/L; (b) 0.04, 0.02mol/L; (c) 0.04, 0.03mol/L; The length of the scale bars is 2µm.
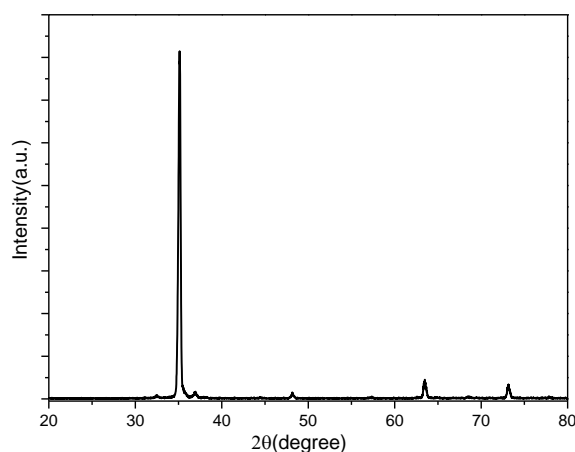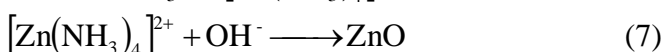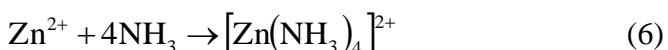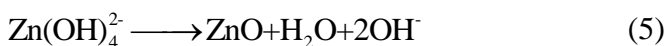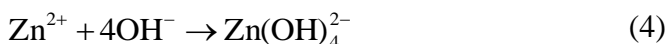

Figure 5. The typical X-ray diffraction patterns of ZnO nanorods.

Fig. 4 showed the diagrams of the multi-branched ZnO nanorods with the concentration changing of $Zn(CH_3COO)_2 \cdot 2H_2O$ and $C_6H_{12}N_4$ were （a）0.04, 0.01mol/L; (b) 0.04, 0.02mol/L; (c) 0.04, 0.03mol/L). As can be seen from the graph, these multi-rod structures originated from a single

nuclei and contained several nanorods branches. When the concentration of reactants was arrived at 0.04 and 0.03 mol/L, ZnO nano-branches were formed correspondingly. It can be seen from the figure, the top section of the bifurcation of the multi-branched ZnO were hexagonal. The samples of crystalline were perfect. These images show the good degree of crystallization of nanorods along the c-axis growth.

Fig. 5 shows the typical X-ray diffraction patterns of ZnO nanorods prepared by solution growth method. It can be seen that the ZnO nanorods have the strongest (002) diffraction peak and narrow FWHM well indexed to the Bragg reflections of the standard wurtzite structure zinc oxide (JCPDS Card File No. 36-1451, a=0.3249nm and c=0.5206nm), indicating that these ZnO nanorods have good crystalline and perfectly oriented growth.

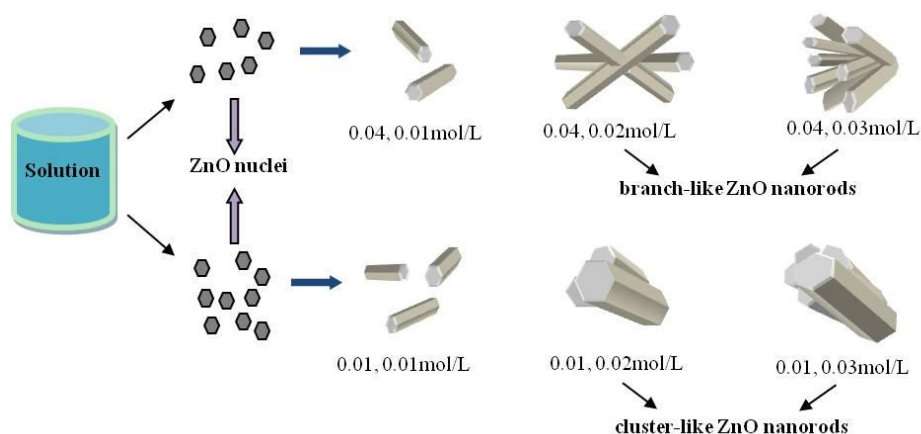The process of formation of ZnO nanorods powders can be represented by the following equations:

$$(CH_2)_6N_4 + 6H_2O \rightarrow 6HCHO + 4NH_3 \tag{1}$$

$$NH_3 + H_2O \rightarrow NH_4^+ + OH^- \tag{2}$$

$$Zn^{2+} + 2OH^- \rightarrow ZnO(nuclei) + H_2O \tag{3}$$

$$Zn^{2+} + 4OH^- \rightarrow Zn(OH)_4^{2-} \tag{4}$$

$$Zn(OH)_4^{2-} \longrightarrow ZnO + H_2O + 2OH^- \tag{5}$$

$$Zn^{2+} + 4NH_3 \rightarrow \left[Zn(NH_3)_4\right]^{2+} \tag{6}$$

$$\left[Zn(NH_3)_4\right]^{2+} + OH^- \longrightarrow ZnO \tag{7}$$

During the forming process of ZnO nanorods, the growth process of ZnO crystalline grains was generally divided into two parts: nucleation and growth. The specific reaction process described as followed: the reactants $Zn(CH_3COO)_2 \cdot 2H_2O$ and $C_6H_{12}N_4$ were hydrolyzed quickly with the increasing of temperature under hydrothermal conditions, resulting in the increasing of the concentration of Zn^{2+} and OH^-, shown in equation (1) and (2) [13-15]. The conditions of supersaturation of Zn^{2+} and OH^- will lead to rapid nucleation, and then form ZnO nuclei, shown in equation (3). The remaining growth units directionally grew around the ZnO nuclei and formed ZnO nanostructures, shown in equation (4) and (5) [16].

In order to investigate the effect of the $C_6H_{12}N_4$ concentration on the morphology of ZnO nanostructures, $C_6H_{12}N_4$ maintained in the higher concentration (0.04mol/L), the concentration of $Zn(CH_3COO)_2 \cdot 2H_2O$ gradually increased, and the other experiment condition, such as the reaction temperature and reaction time were fixed. The basic forming process of ZnO nanoclusters can be explained as follow: when the concentration of $C_6H_{12}N_4$ much greater than the concentration of $Zn(CH_3COO)_2 \cdot 2H_2O$, large amounts of ammonia will be forming. In aqueous solution, ammonia hydrolyzed to NH^{4+} and OH^-, as shown in (2). Due to the high concentration of $C_6H_{12}N_4$, the part of Zn^{2+} and OH^- combine and form the ZnO nuclei, as shown in equation (3), and the formation of ZnO nanorods grow along the c-axis at 90 ^0C. Another part of the Zn^{2+} and the ammonia which produced in equation (1) to form the $[Zn(NH_3)_4]^{2+}$ complex ions, as shown in Equation (6) [21]. It leads to part of the $[Zn(NH_3)_4]^{2+}$ complex ions adsorbed on ZnO nuclei surface[19]. Due to a certain amount of OH^- produced in equation (2), ZnO branches-structure were grown by the reaction of $[Zn(NH_3)_4]^{2+}$ complex ions and OH^-, as shown in (7). The schematic illustration of the formation of

branch-like ZnO and cluster-like ZnO nanorods with different concentration were given in fig 6. By tuning the growth parameters, researchers can efficiently control the structure[22]. The morphology and size of ZnO can importantly influence the optical prosperities, which can be used in the field of solar cell and electrochemistry.

Figure 6. The schematic of the growth process of the formation of branch-like ZnO and cluster-like ZnO nanorods with different concentration.

4. CONCLUSIONS

In summary, one-dimensional ZnO nano-powder with different morphologies can be fabricated by a simple chemical bath deposition. A variety of morphologies of ZnO nanostructures were generated without adding any active agent. The changes of concentration of $Zn(CH_3COO)_2 \cdot 2H_2O$ and $C_6H_{12}N_4$ have an important influence on the ZnO morphology. The photographs revealed that the evolution of ZnO nanostructures from nanorods to dumbbell-shaped and nano-branches. In addition, the growth mechanism of multi-structure ZnO was deeply discussed.

References

1. Niyom Hongsith and Supab Choopun, *Chiang Mai Journal of Science,* 37(2010)48.
2. L. Guo, C. L.Yang, J. N.Wang, S. H.Yang, *Appl. Phys. Lett.*, 76(2000)2901.
3. Rasu Ramachandran, Veerappan Mani, Shen-Ming Chen, George peter Gnana kumar, Pandi Gajendran, Natarajan Biruntha Devi, Rajkumar Devasenathipathy, *Int. J. Electrochem. Sci.*, 10 (2015) 3301.

4. C. Dunkel, M. Wark, T. Oekermann, R. Ostermann, B.M. Smarsly, Electrochim. Acta, 90 (2013) 375.
5. Francisco A. Cataño, Humberto Gomez, Enrique A. Dalchiele, Ricardo E. Marotti, Int. J. Electrochem. Sci., 9 (2014)534.
6. Guang Wei She, Xiao Hong Zhang, Wen Sheng Shi, Xia Fan, Jack C. Chang, Chun Sing Lee, Shuit Tong Lee, and Chang Hong Liu, *Appl. Phys. Lett.*, 92 (2008)053111.
7. J. Y. Park, D. J. Lee, B. T. Lee, J. H. Moon, S. S. Kim, *Journal of Crystal Growth*, 276(2005)165.
8. Y. Sun, G.M. Fuge, M. N. R. Ashfold, *Chem. Phys. Lett.*, 396(2004)21.
9. K. B. Sundaram, A. Khan, *Thin Solid Films*, 295(1997)87.
10. G. Z. Jia, N. Wang, L. Gong, X. N. Fei, *Chalcogenide Letters*, 6 (2009)463.
11. G. Z. Jia, Y. F. Wang, J. H. Yao, *Journal of Ovonic Research*, 6(2010)303.
12. G. Z. Jia, Y. F. Wang, J. H. Yao, *Journal of Physics and Chemistry of Solids*, 73(2012)495.
13. Zhuo Wang, Xue feng Qian, Jie Yin, and Zi kang Zhu, *Langmuir*, 20(2004) 3441.
14. Q. Ahsanulhaq, S. H. Kim, Y. B. Hahn, *Journal of Physics and Chemistry of Solids*, 70(2009) 627.
15. J. Tang, X. R. Yang, *Materials Letters*, 60(2006)3487.
16. J. H. Jang, J. H. Park, S. G. Oh, *Journal of Ceramic Processing Research*, 10(2009) 783.
17. Y. F. Gao, H. Y. Miao, H. J. Luo, and M. Nagai, *Crystal Growth& Design*, 8(2008) 2187.
18. Y. Peng, A. W. Xu, B. Deng, M. Antonietti, and H. Colfen, *J. Phys .Chem. B*, 110(2006) 2988.
19. L. Vayssieres, K. Keis, A. Hagfeldt, and S. E. Lindquist, *J. Chem. Mater.*, 13(2001) 4395.
20. R. A. Laudise, E. D. Kolb, and A. J. Caporaso, *J. Am. Ceram. Soc.*, 47(1964)9.
21. Zhong Lin Wang, *Materials Science and Engineering R*, 64(2009)33.
22. G. Z. Jia, B. X. Hao, X. C. Lu, J. H. Yao, *Int. J. Electrochem. Sci.*, 8(2013)7976.